Use of a high spatial resolution microphone to characterize the early reflections generated by a WFS loudspeaker array

Terence Caulkins[1], Arnaud Laborie[2], Etienne Corteel[1], Remy Bruno[2], Sebastien Montoya[2], and Olivier Warusfel[1]

[1]*IRCAM, 1 Pl. Igor Stravinsky, Paris, FRANCE*

[2]*TRINNOV AUDIO, 30-32 Ave. de la Republique, Villejuif, FRANCE*

Correspondence should be addressed to Terence Caulkins (`terence.caulkins@ircam.fr`)

ABSTRACT

This article deals with a characterization of the early reflections generated by a linear Wave Field Synthesis (WFS) array. Techniques based on the use of planar microphone arrays suffer from an inability to discriminate side-wall reflections from ceiling-floor reflections. An approach combining the use of a high spatial resolution microphone with a geometric model is investigated in order to overcome this problem.

1. INTRODUCTION

A current topic of research in surround sound concerns the application of Wave Field Synthesis to the enhancement of live concert performances, whereby virtual sound sources are rendered on stage alongside real instruments. This juxtaposition of real and virtual sources on stage implies the possibility for the audience to assess the quality of the WFS rendered sound field by direct comparison with a real source sharing the same physical space.

On one hand, the **direct sound field** produced by real sources will be compared to the direct sound field of virtual sources rendered by WFS. Previous research has yielded a content-dependent multi-channel equalization scheme which allows an optimization of the direct sound field within the horizontal plane situated in front of the loudspeaker array [1]. This algorithm, which supposes free field conditions, generates a set of filters to be applied to the loudspeakers in order to produce the best possible least-squares approximation of a real source's direct sound field. The proposed framework also offers the means to render the direct sound fields of virtual sources displaying variable directivity patterns, based on a linear decomposition of the sound field onto a basis of spatial eigenfunctions [2],[3].

On the other hand, the audience will be able to judge the realism of virtual source reproduction by comparing the **room effect associated to real and virtual sources**. Setting aside the case of extended sources, it can be approximated that real instruments on stage will exhibit point source radiation patterns. This is not the case for virtual sources reproduced using a linear WFS array; though their sound field in the horizontal plane may resemble the target source's sound field, the array itself radiates as a finite line source in 3D. This entails a different mode of interaction with the listening room, and differences are to be expected when comparing the room effect associated to a real source and the room effect that is naturally produced by a WFS array.

In [4] a study of the late reverberance component associated to WFS sources is carried out. For a real source radiating sound into a concert hall, the total power emitted by the source above the Schroeder frequency does not depend on its position or orientation. It follows that the late reverberance will remain steady during source movements and rotations on stage. In [4] the authors show that the power emitted by a WFS array is subservient to both positioning and orientation of the virtual source, mainly because of the finite extent of the window through which the source illuminates the listening room. A method is proposed allowing to predict the power associated to a virtual source synthesized by a WFS array for any position and orientation of the source. When directivity and/or spectral characteristics of the transducers cannot easily be modelled, in-situ measurements of the array synthesizing a given virtual source can provide the power estimation through time-frequency analysis proposed in [5].

The goal of the present article is to expose a complimentary characterization of the room effect produced by a WFS array, in which the focus is shifted towards the **early components of the impulse response**. Methods for characterizing the early components of an impulse response using microphone arrays have been developed in the past as tools for auralization [6]. It was shown that a circular array geometry could be used to perform a high order cylindrical harmonic decomposition of the sound field in a concert hall [7]. However when considering 2D microphone arrays the problem of discriminating floor/ceiling reflections from wall reflections arises, as stated in [8]. This discrimination is crucial for proper sound field characterization, since the reflections stemming from the vertical dimension are "re-mapped" upon the 2D plane and can therefore constitute a source of error in the interpretation of the array measurements.

In light of this problem, the authors investigate a new method for characterizing the early components of the room effect associated to a WFS array. This method combines the use of a 3D high spatial resolution microphone array [9] with a simple geometric model of the listening room in order to identify different reflection components. The proposed characterization will focus on the horizontal plane because of its importance in regard to spatial perception. This can be properly done because the use of a 3D array mitigates the influence of vertical components.

The first section of this paper will be dedicated to describing the functionalities of the microphone and how it can be used to extract directional information in a 3D sound field. In the second section, a simple image source model is used to simulate the in-situ measurement of an ideal source and an ideal WFS array by the 3D microphone array placed in the Espace de Projection concert hall in IRCAM. The model is used to analyze the discrepancies that can be found between the early room effect produced by an ideal point source and that produced by a WFS array synthesizing at the same position in the room. In the final section, the results of the simulation are confronted with real measurements of a 48 channel WFS array in the Espace de Projection.

2. DESCRIPTION OF THE HIGH SPATIAL RESOLUTION MICROPHONE ARRAY

2.1. Presentation

The microphone used in this study is a third-order, full-sphere acoustic field microphone, as described in [9]. Its principle is based on the decomposition [10, 11] of an acoustic field $p(r,\theta,\phi,t)$ into a series of Fourier-Bessel coefficients $p_{l,m}(t)$. This decomposition is given in the frequency domain by

$$P(r,\theta,\phi,f) = 4\pi \sum_{l=0}^{\infty} \sum_{m=-l}^{l} P_{l,m}(f)\, j^l\, j_l(kr)\, y_l^m(\theta,\phi) \quad (1)$$

where:

- $k = 2\pi f/c$, c is the speed of sound, approximately 340 m/s,
- $P_{l,m}(f)$ is the Fourier transform of $p_{l,m}(t)$,
- $P(r,\theta,\phi,f)$ is the Fourier transform of $p(r,\theta,\phi,t)$,
- $j_l(x)$ is the spherical bessel fonction of order l [9],
- $y_l^m(\theta,\phi)$ is the spherical harmonic (l,m) [9].

Using this formalism, it is possible to scan the full 3D acoustic field using the discrete set of signals $p_{l,m}(t)$. In real-world applications of this decomposition the series is truncated above a given maximum value for l, which is referred to as the order L of the decomposition.

The Fourier-Bessel coefficients can be interpreted in three different ways, as represented on figure 1:

- a directivity function giving the source distribution in space,
- a field representation that gives the pressure level for any point in space,
- a spectral representation of the amplitude of the Fourier-Bessel coefficients arranged in a triangle.

The microphone used throughout the present article is a third-order Fourier-Bessel microphone, which means that it delivers an estimation of the Fourier-Bessel coefficients of the acoustic field in which it is immersed, up to order 3.

2.2. Principle

The design of the microphone is based on spatial sampling [9]. This general approach considers a microphone consisting in an array of capsules of known characteristics (by measurements or modelling). Each capsule

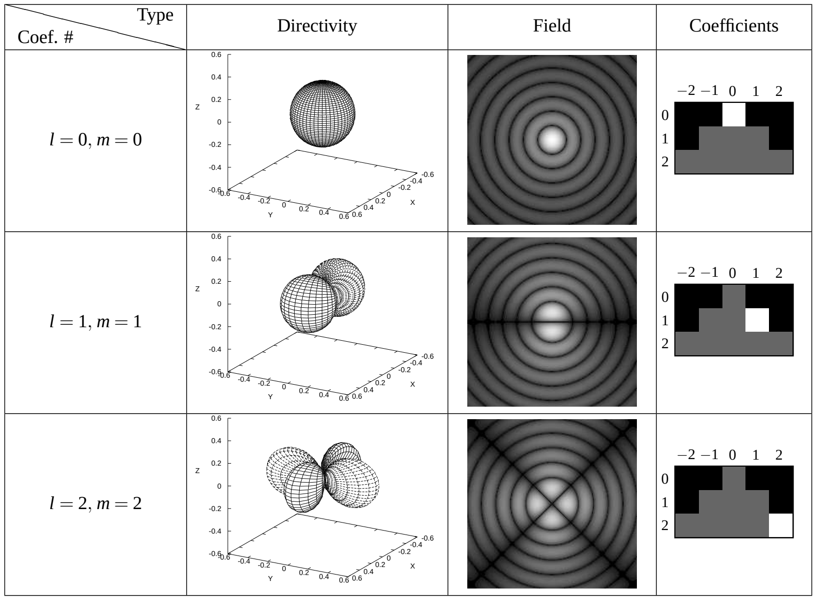

Fig. 1: Various representations of acoustic fields.

extracts a portion of the information contained in the acoustic field to be estimated. This is mathematically represented with the following *sampling relation*, written in the frequency domain:

$$c = Bp \tag{2}$$

where

- B is the *sampling matrix* dependent only on the microphone characteristics (position and directivity of its constituent capsules),
- p is a vector containing the Fourier-Bessel coefficients of the acoustic field being measured,
- c is a vector containing the signals delivered by the capsules.

This matrix relation expresses the fact that it is possible to know the signals delivered by the capsules from the knowledge of the acoustic field in which they are immersed.

Estimation of the Fourier-Bessel coefficients from the capsule signals is the reverse problem of the spatial sampling process. By *inverting* matrix B, it is possible to determine an estimation $\hat{p}$ of the unknown Fourier-Bessel coefficients p from the capsule signals c. This operation is called *encoding* and can be expressed as:

$$\hat{p} = Ec \tag{3}$$

where E is the *encoding matrix*. This matrix can be determined from B using least squares methods, for example. [9] gives a more precise description of the principle of this microphone.

2.3. Spatial resolution of the microphone array

The approach described above allows to design an any-order microphone, provided that the array being used is large enough and contains enough capsules. Trinnov has manufactured a 24-capsule array allowing to reach order 3. The capsules are omnidirectional and irregularly distributed inside a ball of with an approximate diameter of 20 cm.

Acoustic field estimation is not perfect for the following reasons:

- Acoustic field representation is truncated at a given order, here 3. A consequence of this is the limited angular resolution of the resulting directivities. In other words, a plane wave, which is represented in the directivity approach under the form of an angular dirac is not seen as an infinitely narrow source

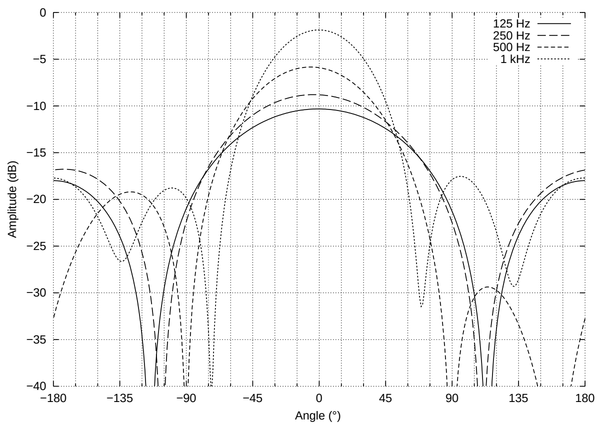

Fig. 2: Angular response of the microphone to a frontal plane wave.

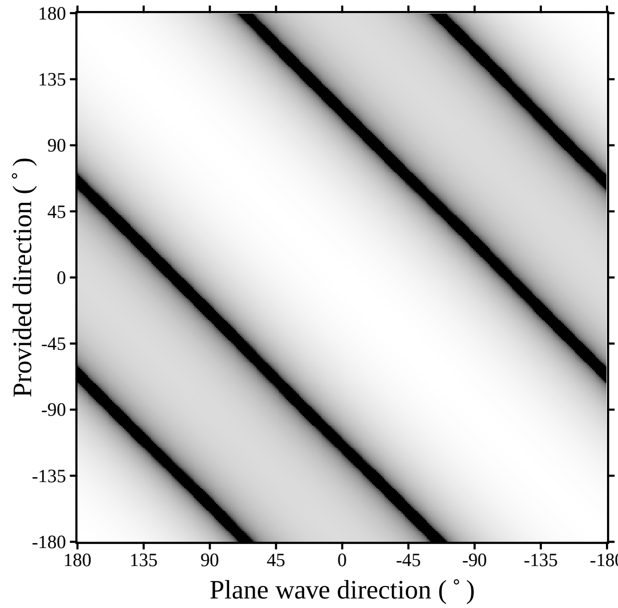

Fig. 3: Directivity transfer matrix of the microphone at 125 Hz.

but as a lobe which has a finite width. Smaller secondary lobes often appear in directions where no source is present.

- The estimation carried out by both the array and the encoding process is not perfect. The 16 coefficients corresponding to the third-order estimated acoustic field do not correspond to the exact 16 first coefficients of the actual acoustic field.
- The microphone array design is not perfect (positions, frequency responses and directivities of the capsules, acoustic masking effect of the array structure…).

Models allow to quantify these imperfections, which depend on frequency. Figure 2 represents the directivity provided by the microphone in the horizontal plane for several frequencies when it captures a plane wave incoming from the front direction. It outlines the better performances of the microphone for medium frequencies than for low frequencies, as the main lobe (around 0˚) is narrower and the secondary lobes are simultaneously smaller. These performances can be represented for incidence directions other than 0˚ and for several frequencies using a matrix representation, as in figures 3, 4, 5 and 6. Each column of this matrix gives the directivity determined by the microphone for a plane wave in a certain direction. The first column is for a source at $+180˚$, the last column is for a source at $-180˚$. The color corresponds to amplitude over 25 dB. Here again, better performances for high frequencies are outlined, as the diagonal, which corresponds to the main lobe, is narrower at 1 kHz, and secondary lobes are lower. An ideal infinite-order microphone would of course have a directivity transfer matrix consisting of ones on its diagonal and zeros everywhere else.

The directivity transfer matrices can be interpreted in two different ways:

- As stated above, each column gives the directivity response that the microphone delivers when it is immersed in a plane wave coming from the direction corresponding to the considered column. Therefore, the curves on figure 2 correspond to the columns labeled 0˚ of the matrices represented on figures 3, 4, 5 and 6.
- Each row corresponds to the directivity of the virtual microphone obtained when the directivity provided by the microphone is spatially sampled in the direction corresponding to the considered row. For example, the signal obtained by considering the value of the directivity, delivered by the microphone, in the direction 0˚ (in the horizontal plane)

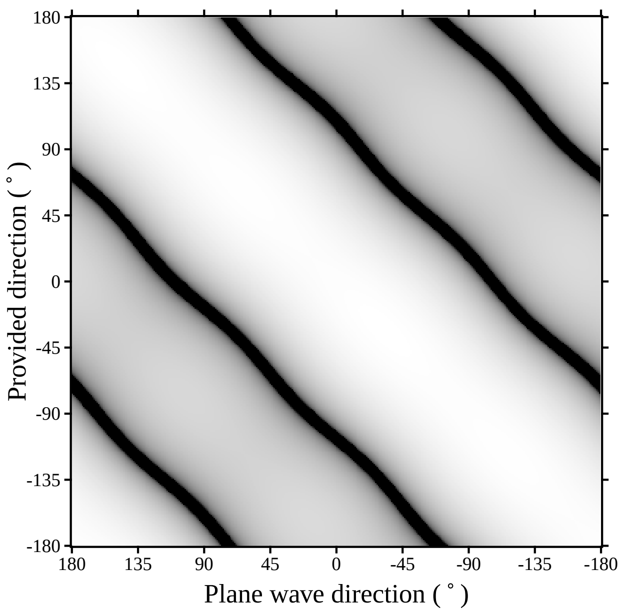

Fig. 4: Directivity transfer matrix of the microphone at 250 Hz.

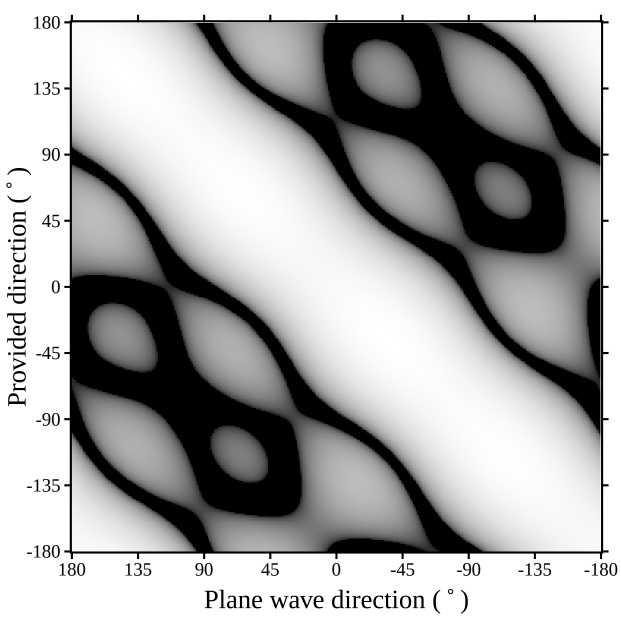

Fig. 5: Directivity transfer matrix of the microphone at 500 Hz.

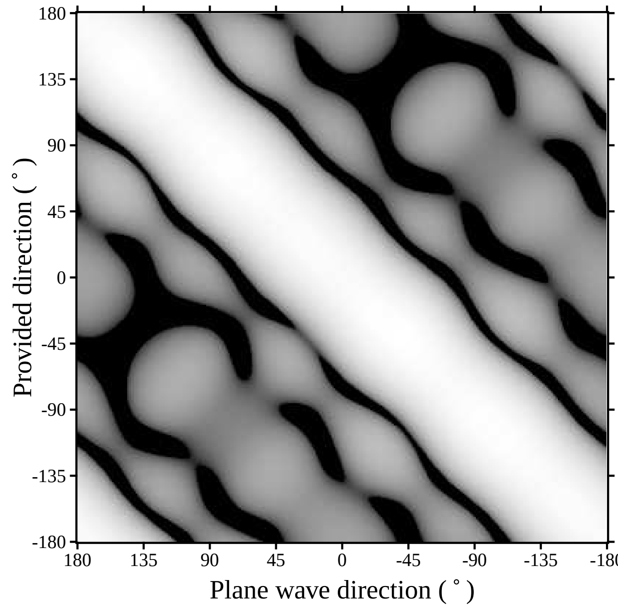

Fig. 6: Directivity transfer matrix of the microphone at 1 kHz.

is the same as the signal delivered by a virtual microphone wich directivity would be the row of the matrix at 0°. On the represented matrices, only the horizontal plane is considered, but the actual directivity of each possible virtual microphone obtained by sampling the provided directivity is three-dimensionnal. Figure 7 gives the virtual directivity at 1kHz obtained by considering the direction 0° in the horizontal plane. The curve labeled *Horizontal* gives the directivity in the horizontal plane while the curve labeled *Vertical* gives the directivity in the vertical plane going through the X-axis (direction 0°). For the vertical curve, 0° is the frontal direction, $+90^\circ$ is the ceiling, $+180^\circ$ and -180 are the back, and -90° is the floor.

3. CHARACTERIZING THE EARLY ROOM EFFECT ASSOCIATED TO A WFS ARRAY FROM SIMULATED MEASUREMENTS MADE ON THE HIGH RESOLUTION MICROPHONE

This section proposes a simulated measurement of the early room effect generated by an ideal source radiating in a rectangular concert hall and the early room effect produced by a WFS array synthesizing the same source.

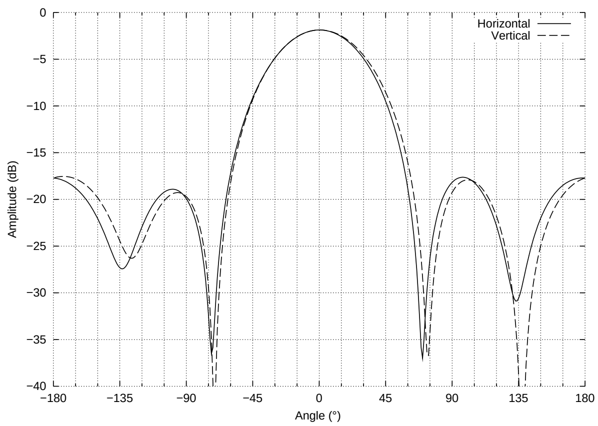

Fig. 7: Directivity obtained at 1kHz by considering the frontal sample of the directivity delivered by the microphone.

The first objective is to verify that the microphone is capable of discriminating specular reflections produced by the ideal source, given a simple image source model of a concert hall. Having verified this, the second objective will be to compare the behavior of the WFS array with that of the ideal source, so as to characterize the particularities of the early room effect that can be associated to virtual WFS sources.

3.1. Description of the simulated measurement setup

The simulated measurement setup involves an ideal source and an ideal WFS array synthesizing the same source at the same position in a rectangular hall that exhibits the same dimensions as the Espace de Projection concert hall in IRCAM ($23.5m(Length) \times 15.5m(Width) \times 11m(Height)$).

The WFS array is modelled as a linear and evenly spaced (16.5cm) distribution of 48 monopole sources. It occupies a central position with respect to the left and right walls, and is situated 5.5m in front of the front wall and 1m78 above the ground (cf figure 8). The virtual source is situated 1m behind the array and 2m to the right of its right bisector.

A characterization of the two sound fields is simulated upon a 24 capsule microphone array exhibiting the same geometrical arrangement as the one described in the previous section. The microphone array is centered at a position situated 5.3m in front of the WFS array and 2.1m to the left of its right bisector, at the same height (1m78 above the ground). An image source model is employed to synthesize the impulse response of the ideal source and the ideal WFS array at the 24 capsule positions. This model will be used in order to help the identification of the various reflections off of the walls of the listening room. Specular reflections (up to the third order image source) are recreated using this model. The walls are modelled with full band, real valued absorption coefficients that approximate the boundary properties of the Espace de Projection during the in-situ measurements described in section 4 (front wall 0.8, left wall 0.001, back wall 0.3, right wall 0.7, floor 0.001, ceiling 0.2).

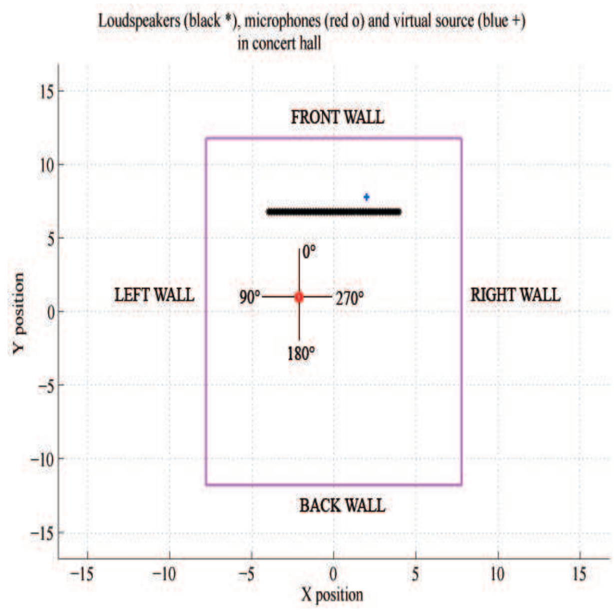

Fig. 8: Configuration for the simulated measurements of an ideal source and a WFS array synthesizing a virtual source at the same position in the concert hall. Source position is represented by a blue cross. Microphone array is represented by a set of red circles. Directional encoding by the microphone is done following a positive angular progression represented on the black axes.

The 24 simulated impulse responses are encoded onto a set of third order spherical harmonics and subsequently decoded in order to form the response of 36 hyperdirectional microphones arranged in the horizontal plane, at 10° intervals (figure 8 shows 4 of the 36 available directions).

3.2. Ideal source measurement

The simulated measurement of an ideal source situated at the position described in figure 8 is carried out on the high spatial resolution microphone and translated into 36 directional responses in the horizontal plane, as described in the previous section. Three ideal sources are considered: a monopole (omnidirectional) source, a dipole source (degree -1 spherical harmonic) and a dipole source with its zero plane perpendicular to the previous one (degree 1 spherical harmonic). The pressure field $p_{ideal}(r,\theta,\phi)$ emitted by the ideal source is based on the far field approximation of a directive point source and described by the following equation:

$$p_{ideal}(r,\theta,\phi) = \frac{e^{-jkr} \cdot cos(n\theta)sin(n\phi)}{r} \tag{4}$$

with n the degree of the source, r the distance from the source, θ the azimuthal angle (contained in the plane parallel to the floor of the hall) and ϕ the polar angle.

The result of the measurement and subsequent directional decoding of the **ideal monopole source** is represented as a function of time on figure 9. Cyan letters are placed at the expected (azimuth, time) coordinates of first and second order reflections according to the image source model applied to the ideal source.[1] :

- Capital letters 'F', 'L', B', 'R', 'G', 'C' represent angular/temporal coordinates of first order reflections off of (resp.) the Front wall, Left wall, Back wall, Right wall, Ground and Ceiling. *Direct sound is represented by a capital 'D'.*

- Lowercase letters represent second order reflections with each letter representing a consecutive reflection off of a given boundary of the listening room. For example, *lg* represents a reflection off of the left wall and then the ground ; *bc* represents a reflection off of the back wall then the ceiling.

- Image sources with identical positions are represented only once. In this configuration we have $gf = fg$, $gl = lg$, $gb = bg$, $gr = rg$, $cf = fc$, $cl = lc$, $cb = bc$, $cr = rc$, $fl = lf$, $fr = rf$, $bl = lb$, and $br = rb$

- Image sources *gc* and *cg* are at different elevation angles. However they present the same (azimuth, time) coordinates so only *gc* is represented.

[1] Image source positions have been slightly shifted in some cases to improve legibility of the figures.

Impulse responses of the ideal source are filtered below 1000Hz, which is the aliasing frequency of the WFS array for the chosen source position at the measurement position (see [3] for an aliasing frequency calculation method taking into account loudspeaker spacing as well as virtual source and listener positioning). This is done in order to be able to compare results with those given for an ideal WFS array in section 3.3.

Observation of figure 9 shows good agreement between the image source model and the directional encoding performed by the microphone array in terms of the expected (azimuth, time) coordinates of first and second order image sources. The monopole source being measured is situated at 340° from the microphone's point of view, as can be seen on figure 8. The direct sound can therefore be expected to arrive from this direction, as is indicated by the cyan 'D' on the figure. The decoded impulse response is properly centered on the expected (azimuth, time) coordinates of the direct sound. The effect of the directivity lobes of the microphone described on figure 2 can be seen to cause a smearing of the impulse response over the azimuthal plane, whereby energy is seen to be incoming from the rear directions as compared to the expected directions of arrival (strictly comprised between angles $[0° - 70°]$ and $[250° - 360°]$). The level of these rear components remains 20dB below the level of direct sound for the $[70° - 250°]$ angular sector. The measured level for the rear components could be made lower by application of a high pass filter on the decoded data (secondary lobes of the microphone are larger for low frequencies, as is visible on figure 2).

Ceiling reflections 'C', *lc*, *rc* and *bc* are greatly diminished (25dB below the direct sound) in comparison to other contributions due to the focussing of the microphone onto the horizontal plane. Ground reflections conserve high levels because of a smaller polar angle of incidence for the first order ground reflection 'G' ($\phi \approx -22°$) compared to the polar angle of incidence for the first order ceiling reflection 'C' ($\phi \approx 42°$), as well as a smaller absorption coefficient of the ground (0.001 vs 0.2 for the ceiling).

In figures 13 (top) and 14 (top), the impulse responses of two **ideal dipole sources** (degree 1 and degree -1) are represented along the 36 incoming directions at the microphone position. The dipole of degree -1 is oriented in such a way that its zero plane encompasses the microphone position. This is visible in the absence of any direct component on figure 13 (top). However, the

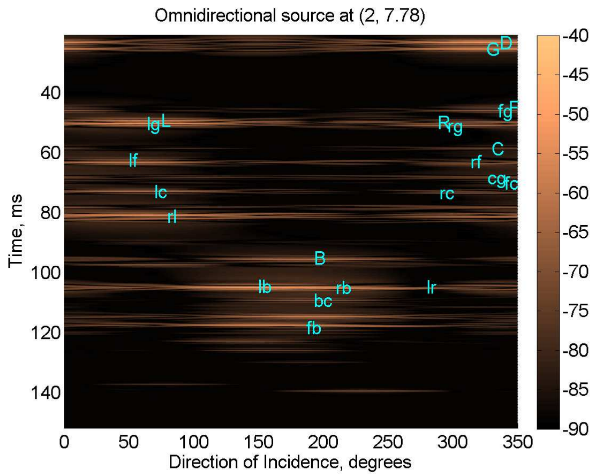

Fig. 9: Amplitude of the impulse response (dB) of an **ideal monopole point source** decoded onto 36 directions (with 10° increments) as a function of time (ms). Cyan letters are placed at the expected (azimuth, time) coordinates of the first and second order reflections according to the image source model for an ideal source (see section 3.2 for details).

same figure shows a strong primary reflection 'L' incoming from the left wall at 70° (at 49.2ms) and a slightly weaker primary reflection 'R' incoming simultaneously from the right wall at 290° as predicted by the image source model. In other words, though the microphone is not illuminated directly by the source, it receives the early reflections produced by the concert hall.

Conversely, the case of the degree 1 dipole shown on figure 14 (top) shows an opposite tendency. This source has its lobe oriented straight at the microphone position. It is therefore observed that the direct sound component (as well as its reflection off the ground) is very strong. However the primary reflection 'L' on the left wall is greatly diminished in comparison with the monopole depicted on figure 9 because this wall receives very little direct sound from the source. The same reasoning can be applied to the second order reflections lc (and cl, not represented) that are extremely attenuated for the degree 1 dipole source (20 dB drop as compared to the monopole source).

3.3. Measurement of an ideal WFS array

In this section the ideal measurements of the ideal point source will be compared with ideal measurements of a WFS array using the setup described in section 3.1.

A set of individual filters needed to be applied to the 48 monopole loudspeaker array in order to synthesize the direct sound field of an ideal point source occupying the same position as the source studied in the previous section is calculated according to the multichannel equalization procedure. Image sources of each individual loudspeaker of the array reflected off of the 6 walls of the listening room are formed in order to construct first, second, and third order 'image arrays'. The individual filters calculated for each loudspeaker are then applied to their corresponding image sources, and the result of the convolution is measured upon the microphone array. Impulse responses are low-pass filtered below the aliasing frequency, calculated to be equal to 1000Hz for this source position.

Figure 12 (top) shows the results of the simulation measurement of the ideal WFS array synthesizing a **virtual monopole point source** at the same position as the ideal source studied in the previous section. The expected image source positions of an ideal point source in the (azimuth, time) plane of the figure are represented in cyan letters. Their positions are strictly identical to those represented on figure 9.

3.3.1. Effect of cylindrical symmetry of the WFS array

A quick scan of figure 12 (top) reveals that certain reflections are slightly delayed compared to their expected time of arrival for an ideal source. This is true for the first order reflections off of the front wall 'F' and ceiling 'C', as well as for second order reflections off of these walls (notably cg and fc). However the direct sound 'D' and first order reflections off of the left wall 'L', right wall 'R' and back wall 'B' display proper arrival times as compared to the ideal source.

To explain this behavior one must take into account the cylindrical geometry of the loudspeaker array. Since each individual source of the loudspeaker array is an ideal monopole, the array displays a cylindrical symmetry around its axis. This in turn implies that the wavefront synthesized for a source situated "behind the array" will be perceived "behind the array" on both sides of the loudspeaker array, as can be seen on figure 10. From this observation, it is clear that the front and back walls receive contributions that arrive with different delays. Since the back wall, left wall and right walls are situated in the targeted reproduction plane they receive contributions that

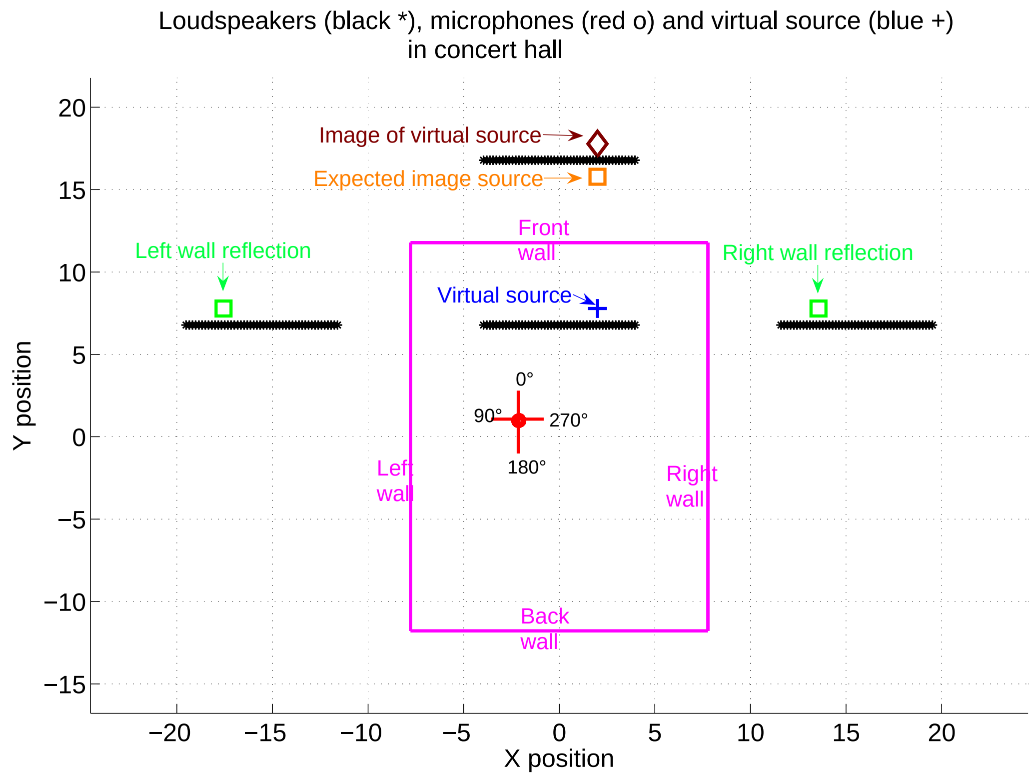

Fig. 11: Illustration of the difference between the expected position of the first order reflection of an ideal source and the actual position of the image of the WFS virtual source. The positions of the image sources associated to left and right walls are correct; however the position of the image source associated to the front wall deviates from the expected position.

remain coherent with the target source position. However, the front wall receives the contribution from a virtual source situated 1m to the other side of the array, i.e. *inside the audience area*, instead of from the expected position situated 1m behind the loudspeaker array (and therefore *outside of the audience area*). This false location of the virtual source also occurs in the vertical direction: the ceiling of the concert hall is in fact illuminated by a wavefront corresponding to virtual source situated 1m *below* the array instead of 1m behind the array in the horizontal plane; the ground of the concert hall receives the contribution from a virtual source situated 1m *above* the array. The consequence of these symmetry errors is that the images of virtual point sources reflected off of the front wall, ceiling and ground are in fact further away than those of the ideal point source. This discrepancy is illustrated in figure 11 for the front reflection. The arrival of the reflections off of these walls is therefore delayed, as can be observed on figure 12 (top).

3.3.2. Variations on the early room effect through directive source synthesis

As stated in the introduction, new developments in WFS allow for the synthesis of virtual sources displaying variable directivity patterns, based on the use of cylindrical harmonics [3]. One of the prescribed goals of this type of directivity rendering can be to approach the directivity patterns of real instruments, as described in [12]. Another interesting prospect offered by directive source rendering lies in the possibility to create *natural variations in the manner in which the loudspeaker array illuminates the concert hall*. In other words, by varying the directivity of a virtual source, one may naturally modify the

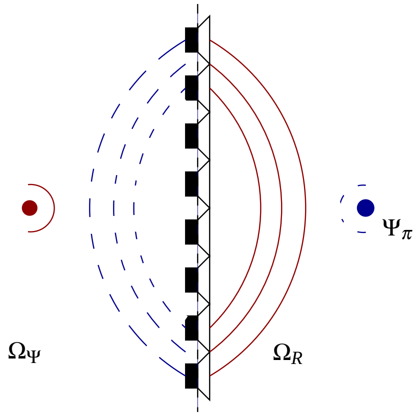

Fig. 10: Illustration of how a given wavefront associated to a source ψ_0 virtually situated in the sub-plane Ω_ψ causes the formation of a symmetrical wavefront corresponding to a virtual source ψ_π situated at a symmetrical position within the sub-plane Ω_ψ

room effect perceived by the audience.

Simulations of the WFS array synthesizing a virtual dipole point source of degree -1 and degree 1 in the model concert hall are shown on figures 13 (middle) and 14 (middle). By comparing the WFS reproduction of the degree -1 dipole (figure 13 middle) with the ideal degree -1 dipole (figure 13 top), it appears that the array is able to recreate the desired attenuation in the direct sound at the microphone position (level of direct sound 'D' 25dB below the level of the primary reflection 'L'). Some artefacts, due notably to the fact that the ground image source 'G' is out of place, remain in the ground reflection component. However, measurements show the possibility for the array to create side reflections while reducing the direct sound. This type of manipulation of the sound field is possible strictly below the aliasing frequency.

The rendering of the degree 1 dipole (figure 14 middle) shows that the lateral reflection 'L' that had been greatly reduced for the ideal source is present for in the array synthesis. This is due to the fact that the zero plane of the degree 1 point source array is not properly reproduced since situated outside of the bounds of the visibility window of the array. Therefore, the primary reflection of the degree 1 source off of the left wall does not exhibit the necessary level attenuation present in the 'L' reflection of figure 14 (top).

The reproduction of a *plane wave* synthesized in a direction perpendicular to the axis of the array and decoded on the microphone array is represented figure 15 (top). It appears first of all that the plane wave source favors the propagation of acoustic energy along the front/back direction (0° and 180°) while reducing the illumination of side walls. Left-wall reflections, which display high levels in the $[20° - 150°]$ angular quadrant for the monopole source, have been strongly attenuated (25dB attenuation of the peak level of the left hand side reflections compared to the 'L' reflection of the monopole source).

Figure 15 (top) also indicates the presence of acoustic energy at the microphone position incoming between 20 and 40 ms within the $[350° - 140°]$ angular sector. This acoustic wave corresponds to the left-wall reflection of the diffracted wave emitted by the sides of the WFS array as the plane wave passes through the finite window of the array. The fact that the diffracted wave is mainly a low frequency phenomenon (below 300Hz) causes an apparent spreading of its angular location since the lobes of the microphone are wider at low frequencies (see figure 2 for frequency dependence of microphone lobes).

4. MEASUREMENTS OF A WFS LOUDSPEAKER ARRAY IN THE ESPACE DE PROJECTION CONCERT HALL

This section describes measurements carried out in the Espace de Projection concert hall in IRCAM using a prototype of the third order microphone array developed by Trinnov. The WFS array is constituted of 48 electrodynamic loudspeakers. The layout of the loudspeakers and microphone array is identical to the one described on figure 8. Results for the measurement of a virtual monopole source, a dipole degree -1 source, a dipole degree 1 source and a plane wave are shown on the bottom of figures 12, 13, 14 and 15. The dynamics of the representation have been greatly reduced in comparison with the specular model (25dB vs 50dB for the ideal simulations) notably because of the presence of measurement noise makes the interpretation of the figures more difficult. The observation of these figures shows a large amount of diffuse energy (absent in the simulations) that appears as a result of the diffusiveness of the walls; however specular components remain more or less coherent with the simulation measurements carried out in the previous section.

Figure 12 (bottom) shows that the main specular components 'D' and 'L' remain coherent with the ideal source for the real-world monopole source reproduction. Synthesis of the degree -1 dipole (fig. 13 bottom) illustrates the potential for cancelling out the direct sound while conserving lateral reflection components using the WFS array. Finally, figure 15 (bottom) shows that the real world array synthesizing a plane wave successfully manages to concentrate acoustic energy in the front-back direction of the concert hall while attenuating reflections incoming from lateral directions at the microphone position.

5. CONCLUSIONS

This article demonstrated the interest of using a high spatial resolution microphone to characterize the early room effect associated to a linear WFS array placed in a concert hall. The array displayed the capacity to reduce contributions originating from outside of the horizontal plane, therefore furnishing the means by which to interpret the measured sound field. The following characteristic aspects of the early room effect associated to a WFS array were underlined:

- Reflections off of surfaces parallel to the axis of the array can be expected to reach the audience area later than expected because of the cylindrical symmetry of the wavefront emitted by the WFS array.
- The synthesis of directive sources allows to create lateral reflections while eliminating the direct sound. The synthesis of plane wave sources allows to accentuate the direct sound level while attenuating lateral reflections. The WFS array can therefore provide a natural means[1] by which to vary the room effect produced within the audience area.

The objective results shown in this study form the potential basis for a perceptual analysis of the early room effect produced by WFS arrays. Objective criteria associated to the perception of room acoustics such as Lateral Energy Fraction and IACC are intrinsically linked to previous microphone technologies (figure 8, dummy head). A topic for further research can be found in the conception of more advanced room acoustics criteria, based on the improved spatial resolution offered by the microphone used in this study.

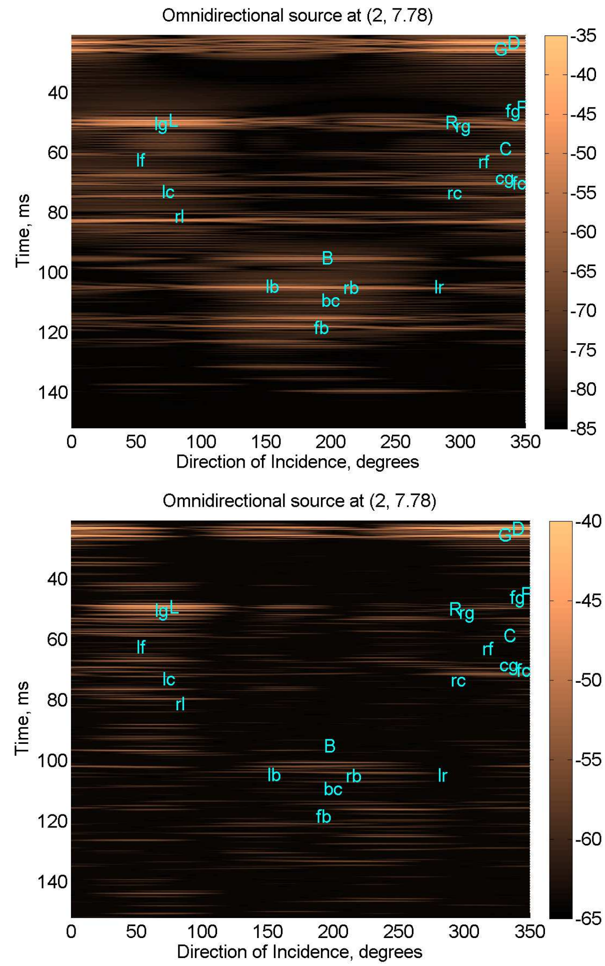

Fig. 12: Amplitude of the impulse response (dB) of a **virtual monopole point source synthesized on the ideal WFS array** (top) and **virtual monopole point source synthesized on the real-world WFS array** (bottom), decoded onto 36 directions at the microphone position (with 10° increments) as a function of time (ms). Cyan letters are placed at the expected (azimuth, time) coordinates of the first and second order reflections according to the image source model for an ideal point source.

6. REFERENCES

[1] Corteel, E., Horbach, U., Pellegrini, R., "Multichannel inverse filtering of multiexciter distributed mode loudspeaker for wave field synthesis." AES 112th Convention, Munich, Germany, May 2002.

[2] Caulkins, T., Corteel, E., Warusfel, O., "Wave field Synthesis interaction with the listening environment, improvements in the reproduction of virtual sources situated inside the listening room." DAFX-03, London, 2003.

[1] Without the use of a dedicated reverberation enhancement system

[3] Corteel, E., “Caracterisation et Extensions de la Wave Field Synthesis en conditions reelles.”, PhD Thesis, Universite Pierre et Marie Curie, 2004

[4] Caulkins, T., Warusfel, O., “Characterization of the Reverberant Sound Field Emitted by a Wave Field Synthesis Driven Loudspeaker Array”, AES 120th Convention, Paris, France, 2006 May 20–23

[5] Jot, J., Cerveau, L., Warusfel, O., “Analysis and synthesis of room reverberation based on a statistical time-frequency model”, AES 103rd Convention, New-York, 1997

[6] Hulsebos, E. and de Vries, D. and Bourdillat, E., “Improved microphone array configurations for auralization of sound fields by wave field synthesis”,AES 110th Convention, Amsterdam, Netherlands, May 2001

[7] Hulsebos, E., “Auralization using Wave Field Synthesis”, PhD Thesis, TU Delft, Delft, Netherlands, 2004

[8] Spors, S. and Buchner, H. and Rabenstein, R., “Efficient Active Listening Room Compensation for Wave Field Synthesis”, AES 116th convention, Berlin, Germany, 2004

[9] Laborie, A., Bruno, R., Montoya, S. “A New Comprehensive Approach of Surround Sound Recording”, AES 114th, Amsterdam, The Netherlands, 2003 March 22–25.

[10] Michel Bruneau. *Manuel d’acoustique fondamentale*. Hermes, 1998.

[11] E. Skudrzyk. *The Foundations of Acoustics: Basic Mathematics and Basic Acoustics*. Springer-Verlag, 1971.

[12] Warusfel, O. and Corteel, E. and Misdariis, N. and Caulkins, T., “Reproduction of sound source directivity for future audio applications”, ICA04, Kyoto, Japan, 2004

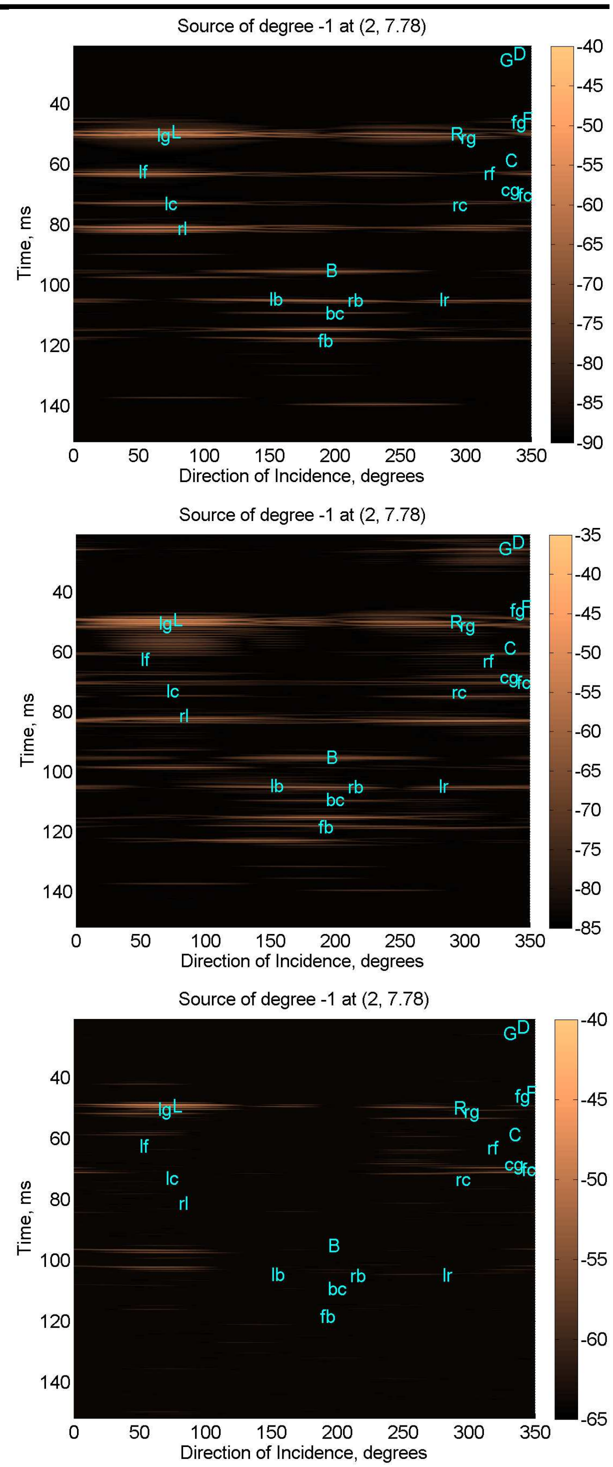

Fig. 13: Amplitude of the impulse response (dB) of an **ideal dipole point source of degree -1** (top), **virtual dipole point source of degree -1 reproduced on an ideal WFS array**(middle) and **virtual dipole point source of degree -1 reproduced on the real-world WFS array** (bottom), decoded onto 36 directions by 10° increments as a function of time (ms).

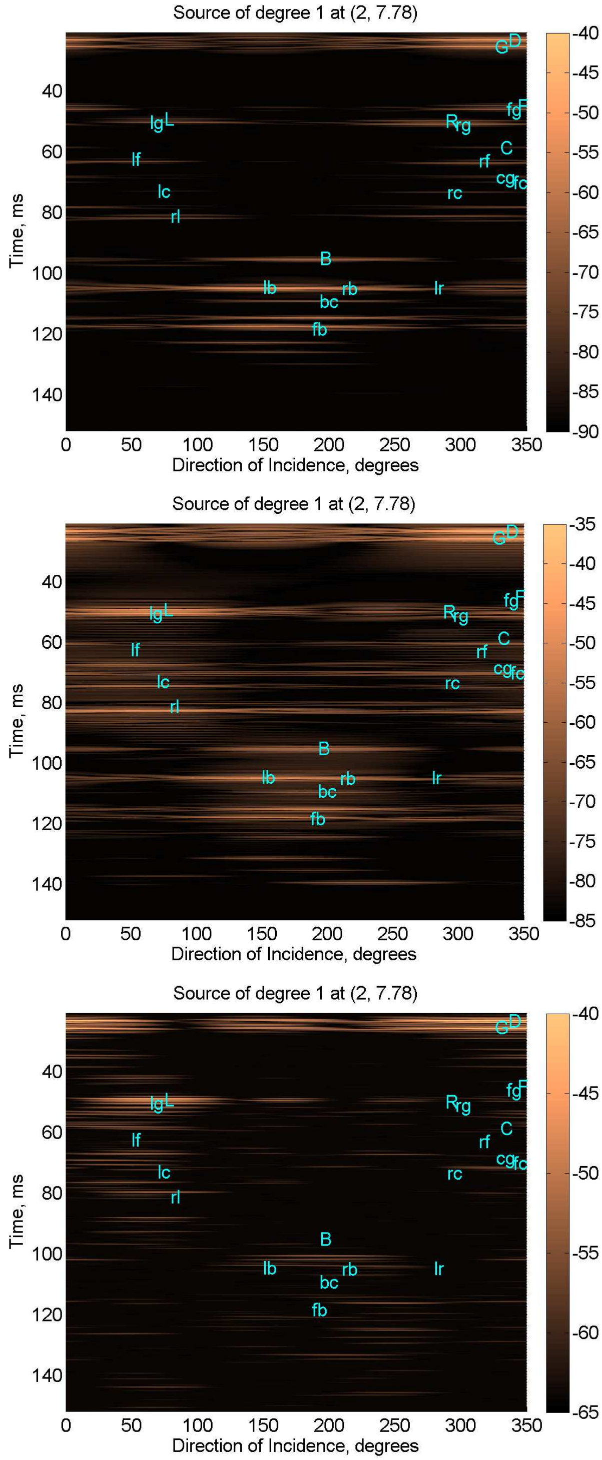

Fig. 14: Amplitude of the impulse response (dB) of an **ideal dipole point source of degree 1** (top), **virtual dipole point source of degree 1 reproduced on an ideal WFS array**(middle) and **virtual dipole point source of degree 1 reproduced on the real-world WFS array** (bottom), decoded onto 36 directions by 10° increments as a function of time (ms).

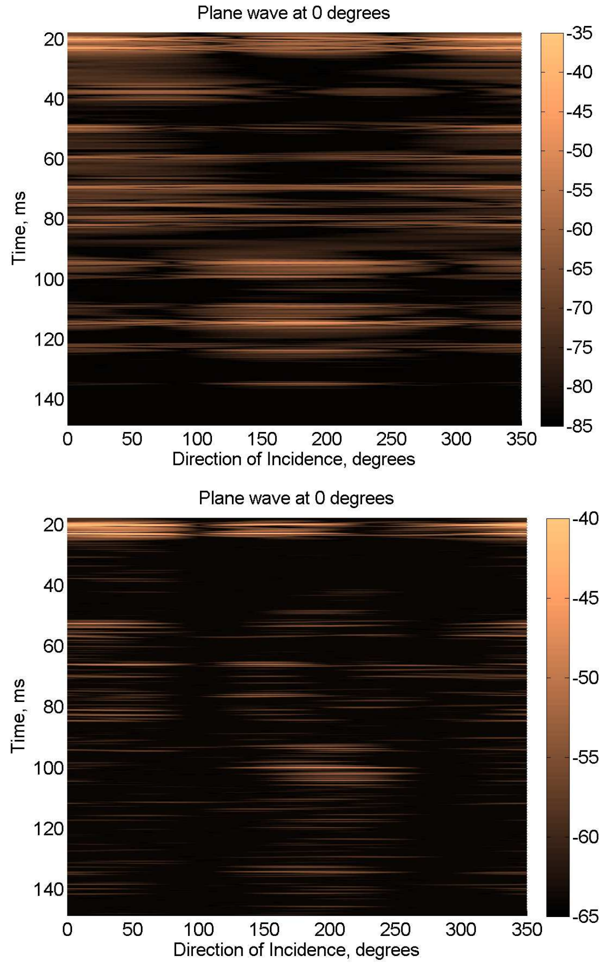

Fig. 15: Amplitude of the impulse response (dB) of a **virtual plane wave synthesized in a direction perpendicular to the axis of the ideal WFS array** (top) and **virtual plane wave synthesized in a direction perpendicular to the axis of the real-world WFS array** (bottom), decoded onto 36 directions at the microphone position (with 10° increments) as a function of time (ms).